Inorg. Chem. **2006**, *45*, 6706–6712

Synthesis and Characterization of Imidocubanes with Exocube Ge^{IV} and Sn^{IV} Substituents: $[M(\mu_3\text{-}NGeMe_3)]_4$ (M = Sn, Ge, Pb); $[Sn(\mu_3\text{-}NSnMe_3)]_4$

Jack F. Eichler,*[,†,‡] Oliver Just,[‡,§] and William S. Rees, Jr.[‡]

Division of Natural Science and Mathematics, Oxford College of Emory University, Oxford, Georgia 30054, School of Chemistry and Biochemistry, Oberlin College, Oberlin, Ohio 44074, and School of Chemistry and Biochemistry and School of Materials Science and Engineering and Molecular Design institute, Georgia Institute of Technology, Atlanta, Georgia 30332-04000

Received February 27, 2006

The heteroleptic lithium amide, $[(Me_3Sn)(Me_3Ge)NLi\cdot(Et_2O)]_2$ (**2**), reacts with MCl_2 (M = Sn, Ge, Pb) to yield the corresponding cubane complexes $[M(\mu_3\text{-}NGeMe_3)]_4$ [M = Sn (**3**), Ge (**4**), Pb (**5**)]. In an analogous reaction with $SnCl_2$, the lithium stannylamide, $[(Me_3Sn)_2NLi\cdot(Et_2O)]_2$ (**1**), produces the mixed-valent Sn congener $[Sn(\mu_3\text{-}NSnMe_3)]_4$ (**6**). All imidocubanes contain both di- and tetravalent group 14 metals that are bridged by N. These structures are comprised of M_4N_4 (M = Sn, Pb, Ge) cores that possess varying distortion from perfect cube geometry. The Pb derivative (**5**) exhibits enhanced volatility and vapor-phase integrity.

Introduction

The initial report on the preparation of the tin−nitrogen heterocubane, $[SnNC(CH_3)_3]_4$,[1] provided access to a class of compounds possessing a unique bonding environment around the divalent Sn atom. A number of homologous complexes containing various alkyl substituents have since been synthesized,[2] and a number of investigations have subsequently aimed to facilitate oxidation of the Sn center.[3,4] Though significant progress has been made in understanding the nature of this class of tin compounds, little has been done to extend the identity of exocube moieties beyond carbon and only a handful of germanium and lead congeners have been reported.[5−7]

During our ongoing effort to explore the chemistry of lithium stannylamide, $[(Me_3Sn)_2NLi\cdot(THF)]_2$ (**1**), and its mixed silyl−stannyl derivative, $[(Me_3Sn)(Me_3Si)NLi\cdot(Et_2O)]_2$, a new route to imidocubanes was recently reported.[8] This pathway proceeds via the reaction of lithium (trimethylsilyl)(trimethylstannyl)amide and the appropriate divalent metal chloride, and a series of heterocubane compounds $\{[M(\mu_3\text{-}NSiMe_3)]_4$ (M = Ge, Sn, Pb)$\}$ has been prepared in this fashion (Scheme 1).[8,9] The elimination of trimethyltin chloride is thought to constitute the driving force for the formation of these heterocubanes and is believed to involve in situ generation of an imidotin(II) intermediate and eventual tetramerization of the M−N core (a discussion of the potential mechanism of tin(II) imidocubane formation has been previously published).[10] This route to group 14 heterocubanes differs from previously reported syntheses, which include the reaction of magnesium imides with metal halides[5] and the reaction of primary amines with metallocene complexes,[6] metal amides,[10] and cyclic diazastannylenes.[11] In addition, a recent report by Kemp et al. describes the synthesis of a

* To whom correspondence should be addressed. E-mail: jack.eichler@emory.edu.
† Oxford College of Emory University.
‡ Georgia Institute of Technology.
§ Oberlin College.

(1) Veith, M.; Sommer, M. L.; Jager, D. *Chem. Ber*. **1979**, *112*, 2581−2587.
(2) Veith, M. *Chem. Rev.* **1990**, *90*, 3−16.
(3) Chivers, T.; Clark, T. J.; Krahn, M.; Parvez, M.; Schatte, G. *Eur. J. Inorg. Chem*. **2003**, 1857−1860.
(4) Chivers, T.; Clark, T. J.; Parvez, M.; Schatte, G. *Dalton Trans*. **2003**, 2107−2108.
(5) Grigsby, W. J.; Hascall, T.; Ellison, J.; Olmstead, M. M.; Power, P. P. *Inorg. Chem.* **1996**, *35*, 3254−3261.
(6) Allan, R. E.; Beswick, M. A.; Davies, M. K.; Raithby, P. R.; Steiner, A.; Wright, D. S. *J. Organomet. Chem.* **1998**, *550*, 71−76.
(7) Chen, H.; Bartlett, R. A.; Dias, H. V. R.; Olmstead, M. M.; Power, P. P. *Inorg. Chem.* **1991**, *30*, 3390−3394.
(8) Eichler, J. F.; Just, O.; Rees, W. S., Jr. *Phosphorus, Sulfur, Silicon Relat. Elem.* **2004**, *179(4−5)*, 715−726. The crystal structure of compound **1**, previously unreported, is included in the Supporting Information.
(9) Eichler, J. F.; Just, O.; Rees, W. S., Jr. In *Modern Aspects of Main Group Chemistry*; ACS Symposium Series 917; Lattman, M., Kemp, R. A., Eds.; Oxford University Press: New York, 2005; pp 123−137.
(10) Bashall, A.; Feeder, N.; Harron, E. A.; McPartlin, M.; Mosquera, M. E. G.; Saez, D.; Wright, D. S. *J. Chem. Soc., Dalton Trans.* **2000**, 4104−4111.
(11) Veith, M.; Opsolder, M.; Zimmer, M.; Huch, V. *Eur. J. Inorg. Chem.* **2000**, *6*, 1143−1146.

10.1021/ic060331y CCC: $33.50
Published on Web 07/21/2006

Scheme 1

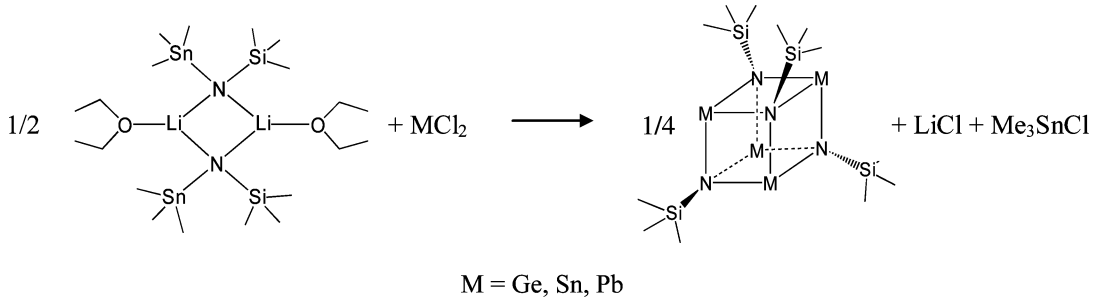

Scheme 2

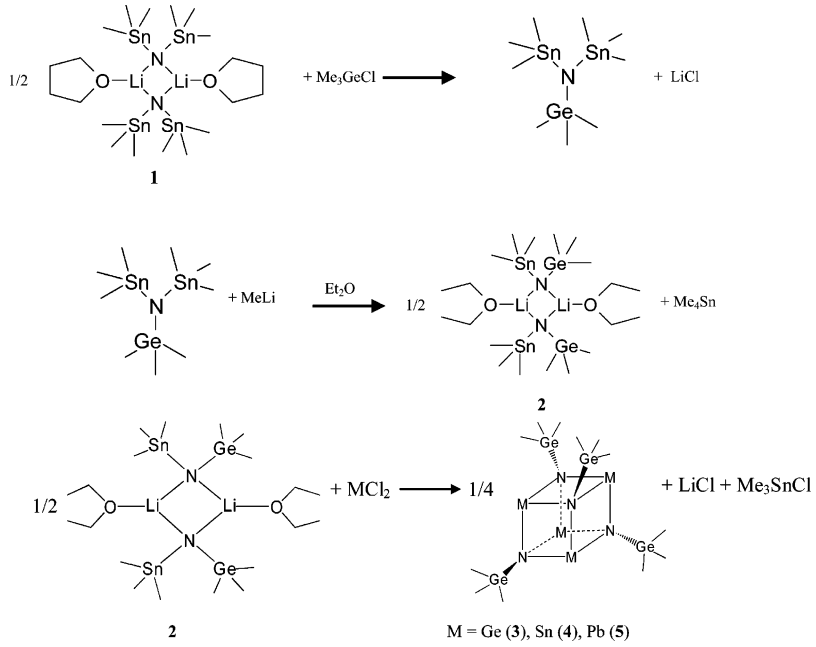

Scheme 3

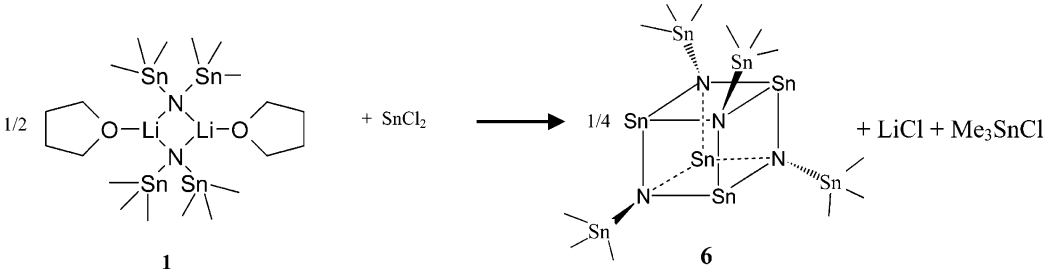

tin−nitrogen cubane via the reaction of tin(II) chloride and a lithiated secondary amine possessing an extremely bulky functional group.[12]

In view of the potential employment of group 14 heterocubanes as precursors for IV−VI semiconductor materials[3] and the general suitability of metal amide compounds in metal−organic chemical vapor deposition (MOCVD) processes,[13,14] it was of interest to expand synthetic access to this class of compounds. To confirm the assumption that control over the exocube substituents in cubane species can be exercised using synthetically modified versions of various lithium amide species, the (trimethylgermyl)(trimethylstannyl) lithium amide complex (**2**) was reacted with a suitable metal dichloride MCl_2 (M = Sn, Ge, Pb; Scheme 2). In addition, to further demonstrate the general utility of this synthetic pathway, a mixed-valent tin imidocubane, possessing exocube trimethylstannyl substituents, was synthesized utilizing the homoleptic lithium stannylamide **1** (Scheme 3). All complexes were characterized using X-ray diffraction, standard spectroscopic and mass spectrometry techniques, and elemental analysis.

Experimental Details

General Procedures. All manipulations were carried out in a dry glovebox atmosphere or by using standard Schlenk techniques.

(12) Tang, Y.; Zakharov, L. V.; Rheingold, A. L.; Kemp, R. A. *Inorg. Chim. Acta* **2006**, *359*, 775−781.
(13) Just, O.; Rees, W. S., Jr. *Adv. Mater. Opt. Electron.* **2000**, *10*, 213.
(14) Eichler, J. F.; Just, O.; Rees, W. S., Jr. *J. Mater. Chem.* **2004**, *14*, 3139−3143.

All solvents were dried over Na^0 or P_2O_5 (CH_2Cl_2) and freshly distilled under an inert atmosphere prior to use. $SnCl_2$, $PbCl_2$, and Me_3GeCl were purchased from Alfa Aesar and used without further purification. Compound **1**[8] and $GeCl_2$·(dioxane)[15] were prepared according to literature procedures. All NMR experiments were performed on a Bruker 400-MHz spectrometer at 300 K using C_6D_6 as the solvent, which was distilled over CaH_2 and stored under argon. ^1H (400-MHz) and ^{13}C (100.6-MHz) NMR spectra were referenced to tetramethylsilane (TMS). ^{119}Sn (149.3-MHz) and ^7Li (155.5-MHz) NMR spectra were externally referenced to Me_4Sn and LiBr, respectively. Elemental analyses were recorded on a Perkin-Elmer series II CHNS/O analyzer 2400, FT-IR measurements were carried out on a Bruker Equinox 55 spectrometer, mass spectrometry analyses were completed on a VG Instruments 70SE (electron impact, 70 eV), and UV/vis measurements were performed on a Perkin-Elmer UV/vis/near-IR Lambda 19 spectrometer. All thermogravimetric analysis (TGA) experiments were registered on a Perkin-Elmer 7/DX thermal analyzer housed in a dry glovebox atmosphere and interfaced to a Perkin-Elmer thermal analysis controller. Argon was used as the purge gas, and all percent weight vs temperature profiles were obtained at a 10 °C/min temperature ramp under ambient pressure. All X-ray diffraction experiments were performed on a Siemens SMART CCD diffractometer using a Mo Kα radiation ($\lambda = 0.710\ 73$ Å) source. All X-ray structures were solved by direct methods (*SHELXS-97*)[16] and refined by full-matrix least-squares procedures (*SHELXL-97*);[17] Lorentz polarization and absorption (*SADABS*) corrections were applied.

[(Me_3Sn)(Me_3Ge)NLi·(Et_2O)]$_2$ (2). Me_3GeCl (1.65 g, 10.80 mmol) was added dropwise to a solution of **1** (4.55 g, 5.40 mmol) in diethyl ether (40 mL) at 0 °C. After stirring overnight at ambient conditions, LiCl was filtered off to give a clear and colorless solution. MeLi (10.80 mmol, 6.75 mL of 1.6 M hexane) was subsequently added under vigorous stirring at −30 °C. After stirring overnight at room temperature, the volume of the reaction mixture was reduced in vacuo to ca. 30 mL and colorless crystals were grown at −40 °C over a 2-day period. Yield: 2.22 g (55%). ^1H NMR: δ 0.23 (s, 18H, CH_3Sn), 0.42 (s, 18H, CH_3Ge), 1.03 (t, 12H, CH_3), 3.39 (q, 8H, CH_2). ^{13}C NMR: δ −1.52 (s, CH_3Sn), 6.96 (s, CH_3Ge), 14.85 (s, CH_3), 64.64 (s, CH_2). ^{119}Sn NMR: δ 46.7 (s, Me_3Sn). ^7Li NMR: δ 1.66 (s). Elem anal. Calcd for $C_{20}H_{56}N_2O_2Li_2Ge_2Sn_2$: C, 31.89; H, 7.49; N, 3.72. Found: C, 32.16; H, 7.11; N, 4.73.

[Ge(μ_3-NGeMe$_3$)]$_4$ (3). A total of 0.60 g of **2** (0.80 mmol), dissolved in 40 mL of diethyl ether, was added to a diethyl ether slurry of $GeCl_2$·(dioxane) (0.23 g, 1.6 mmol) in a dropwise fashion at 0 °C. After stirring overnight at ambient conditions, LiCl was filtered off and the solvent was removed in vacuo. The pale-yellow residue was redissolved in 15 mL of CH_2Cl_2, and pale-yellow crystals were grown at −80 °C over a 2-day period. Yield: 0.05 g (15%). Mp (dec): 265 °C. ^1H NMR: δ 0.50 (s, $GeCH_3$). ^{13}C NMR: δ −1.14 (s, $GeCH_3$). MS (EI, 274 °C): *m*/*z* 820 [M^+]. IR (Nujol): 1261 (m), 1231 (m), 1015 (s), 824 (m), 735 (m), 603 (m), 558 (m) cm^{-1}. Elem anal. Calcd for $C_{12}H_{36}N_4Ge_8$: C, 17.62; H, 4.44; N, 6.86. Found: C, 17.74; H, 4.34; N, 7.34.

[Sn(μ_3-NGeMe$_3$)]$_4$ (4). The synthesis was performed in a fashion analogous to that of compound **3** by reacting **2** (0.50 g, 0.66 mmol) and $SnCl_2$ (0.25 g, 1.33 mmol). Yellow crystals were grown from CH_2Cl_2 at −80 °C over a 2-day period. Yield: 0.07 g (21%). Mp (dec): 250 °C. ^1H NMR: δ 0.45 (s, $GeCH_3$). ^{13}C NMR: δ 0.21 (s, $GeCH_3$). ^{119}Sn NMR: δ 954 (s). MS (EI, 270 °C): *m*/*z* 1002 [M^+]. IR (Nujol): 1075 (m), 818 (m), 725 (m), 599(s), 563 (m), 515 (m) cm^{-1}. Elem anal. Calcd for $C_{12}H_{36}N_4Sn_4Ge_4$: C, 14.39; H, 3.62; N, 5.59. Found: C, 14.41; H, 3.22; N, 5.71.

[Pb(μ_3-NGeMe$_3$)]$_4$ (5). The synthesis was performed in a fashion analogous to that of compound **3** by reacting **2** (0.50 g, 0.66 mmol) and $PbCl_2$ (0.37 g, 1.33 mmol). Yellow crystals were grown from a CH_2Cl_2 solution at −80 °C over a 2-day period. Yield: 0.25 g (55%). Mp (dec): 260 °C. ^1H NMR: δ 0.19 (s, $GeCH_3$). ^{13}C NMR: δ −1.02 (s, $GeCH_3$). MS (EI, 42 °C): *m*/*z* 1356 [M^+]. IR (Nujol): 1228 (m), 812 (m), 719 (m), 589 (m), 531 (w) cm^{-1}. Elem anal. Calcd for $C_{12}H_{36}N_4Pb_4Ge_4$: C, 10.63; H, 2.68; N, 4.13. Found: C, 10.57; H, 2.61; N, 4.22.

[Sn(μ_3-NSnMe$_3$)]$_4$ (6). The synthesis was performed in a fashion analogous to that of compound **3** by reacting **1** (0.50 g, 0.59 mmol) and $SnCl_2$ (0.22 g, 1.19 mmol). Orange crystals were grown from CH_2Cl_2 at −80 °C over a 2-day period. Yield: 0.18 g (51%). Mp (dec): 210 °C. ^1H NMR (400 MHz, C_6D_6, 25 °C, TMS): δ 0.29 (s, $SnCH_3$). ^{13}C NMR (100.6 MHz, C_6D_6, 25 °C, TMS): δ 1.36 (s, $SnCH_3$). ^{119}Sn NMR (149.3 MHz, C_6D_6, 25 °C, Me_4Sn): δ −40.4 (s, $SnMe_3$), 797 (s, Sn(μ_3-N)). MS (EI, 273 °C): *m*/*z* 1188 [M^+]. IR (Nujol): 1181 (w), 1033 (m), 721 (m), 663 (m), 529 (w) cm^{-1}. Elem anal. Calcd for $C_{12}H_{36}N_4Sn_8$: C, 12.15; H, 3.06; N, 4.72. Found: C, 11.96; H, 2.78; N, 3.96.

Results and Discussion

The heteroleptic lithium amide **2** was isolated via the in situ reaction of the amine intermediate, $(Me_3Sn)_2N(GeMe_3)$, with methyllithium, followed by subsequent recrystallization from the reaction solvent. Treatment of **2** with the appropriate divalent metal chloride MCl_2 (M = Ge, Sn, Pb) in a 2:1 ratio produced germanium(II) (**3**), tin(II) (**4**), and lead(II) (**5**) imidocubanes possessing trimethylgermyl substituents. The tetranuclear molecular compositions of complexes **3**−**5** were revealed by X-ray studies to be isostructural, based on the M_4N_4 architecture (see Figures 1−3). Each N atom is four-coordinate, bridging three divalent metal centers (Ge, Sn, or Pb) and one tetravalent Ge center. The M−N cage exhibits the typical distortion from perfect cube geometry, evidenced by the endocubic M−N−M and N−M−N angles (Tables 1−5). The average Ge^{IV}−N interatomic distances of 1.870(9), 1.860(12), and 1.850(2) Å (observed for **3**−**5**, respectively) are slightly longer than the previously reported value found in $(Li[N(GeMe_3)_2])_3$ [Ge−N_{avg} = 1.837(2) Å].[10] The weaker Ge^{IV}−N interactions in **3**−**5** presumably arise because of the presence of three M^{II}−N linkages, compared with only two Li−N interactions in $(Li[N(GeMe_3)_2])_3$. The apparent trend of decreasing Ge^{IV}−N interatomic distances is observed in correlation with weakening endocube M−N interactions. The M^{II}−N interatomic distances are in agreement with previously reported group 14 M−N heterocubanes, with bulky exocube substituents often resulting in longer M−N distances: **3** [Ge−N = 2.002(4) Å] {[GeN(C_6H_6)]$_4$ [Ge−N_{avg} = 2.023(2) Å]},[5] **4** [Sn−N = 2.207(3) Å] {[Sn(μ_3-NSiMe$_3$)]$_4$, 2.196(4) Å;[8,18] [Sn(μ_3-N{4-MeOC_6H_6})]$_4$,

(15) Fjeldberg, T.; Haaland, A.; Schilling, B. E. R.; Lappert, M. F.; Thorne, A. J. *J. Chem. Soc., Dalton Trans.* **1986**, *8*, 1551−1560.
(16) Sheldrick, G. M. *SHELXS 97, Program for Crystal Structure Determination*; University of Göttingen: Göttingen, Germany, 1997.
(17) Sheldrick, G. M. *SHELXL 97, Program for Crystal Structure Determination*; University of Göttingen: Göttingen, Germany, 1997.
(18) Veith, M.; Opsolder, M.; Zimmer, M.; Huch, V. *Eur. J. Inorg. Chem.* **2000**, 1143−1146.

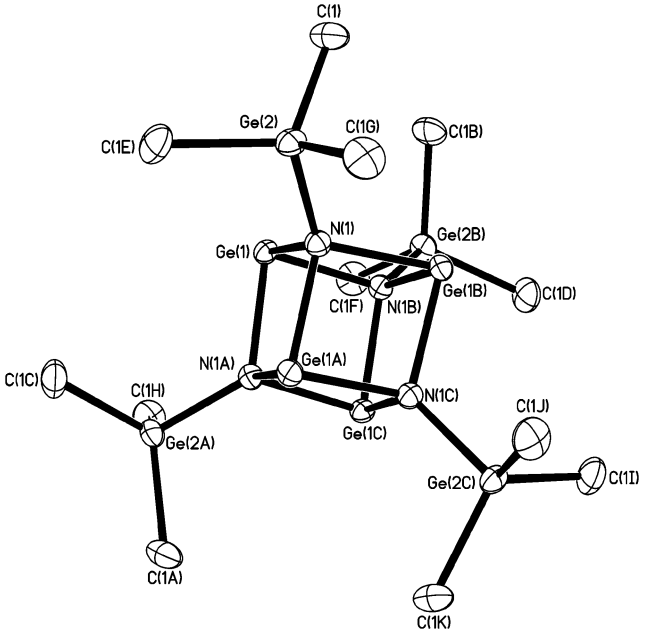

Figure 1. ORTEP plot representation (30% probability) with a numbering scheme for compound **3**. H atoms have been omitted for clarity.

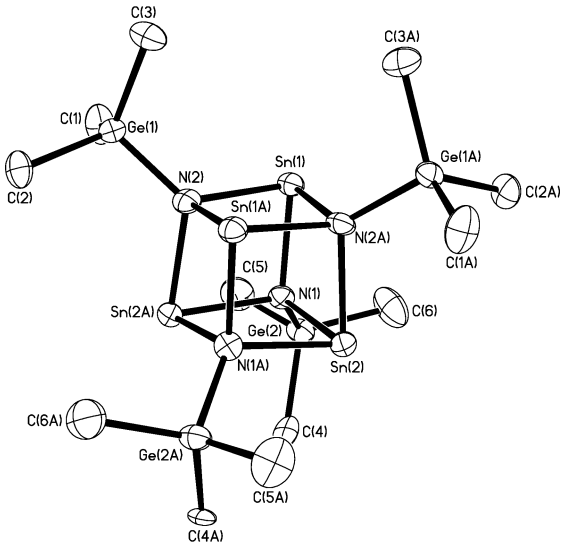

Figure 2. ORTEP plot representation (30% probability) with a numbering scheme for compound **4**. H atoms have been omitted for clarity.

2.205(3) Å;[10] [Sn(μ_3-N{2,6-*i*-$Pr_2C_6H_3$})]$_4$, 2.227(8) Å]},[7] **5** [Pb−N = 2.293(2) Å], [PbN(C_6H_{12})]$_4$ [Pb−N = 2.303(3) Å],[6] and [PbN(2,6-*i*-$Pr_2C_6H_3$)]$_4$ [Pb−N = 2.337(3) Å].[7] Examination of the M−N angles within the central core reveals increasing levels of distortion from perfect cube geometry for the heavier group 14 elements. This can be attributed to the decrease in propensity to participate in sp^3 hybridization displayed by the heavier congeners.[2]

In the crystal structure of **2** (Figure 4), the Sn and Ge atoms were found to be crystallographically indistinguishable. The observed interatomic distances were identical [1.915(2) Å] for all Sn−N and Ge−N interactions. These values lie between the corresponding interatomic distances recorded in the structurally analogous compounds: [(Me_3Sn)$_2$NLi·(*t*-BuMeO)]$_2$, Sn−N_{avg} = 2.093(4) Å,[19] and [LiN($GeMe_3$)$_2$]$_3$, Ge−N_{avg} = 1.837(3) Å.[20] The presence of Ge in the

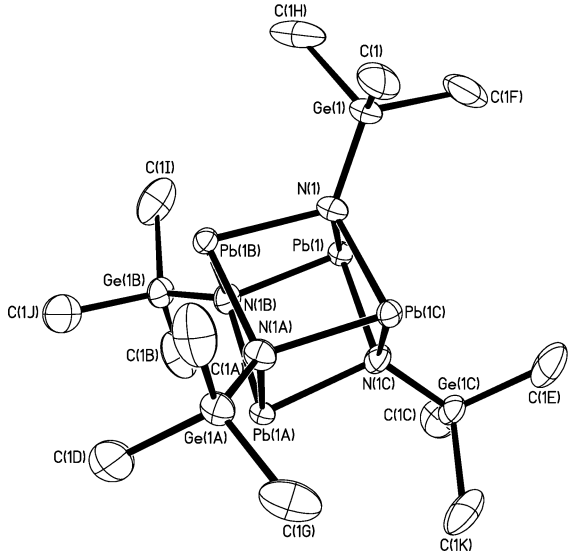

Figure 3. ORTEP plot representation (30% probability) with a numbering scheme for compound **5**. H atoms have been omitted for clarity.

heteroleptic germylstannyllithium amide **2** was confirmed by ^{119}Sn NMR {change in the chemical shift from δ 63.3 for [(Me_3Sn)$_2$NLi·(THF)]$_2$[8] to δ 46.7 in **2**} and elemental analysis.

To further illustrate the synthetic utility of this route to group 14 imidocubanes, the homoleptic lithium stannylamide **1** was reacted with $SnCl_2$ in a fashion similar to that described for **3**−**5**. The mixed-valent cubane **6** (Figure 5) displays average Sn−N endocube distances of 2.196(3) Å, practically identical with those registered in [Sn(μ_3-N$SiMe_3$)]$_4$ [2.196-(4) Å][8,18] and in complex **4**, bearing trimethylgermyl exocube substituents [2.207(3) Å]. The geometry about the Sn^{IV} atoms is distorted tetrahedral, and the average Sn−N interatomic distance of 2.043(7) Å is in agreement with previously reported Sn^{IV}−N distances found in SnBr[N($SiMe_3$)$_2$]$_3$ [2.056(7) Å],[21] Sn(CH_3)(NRAr)$_3$ [R = $C(CD_3)_2CH_3$, Ar = 3,5-$C_6H_3Me_2$; 2.044(4) Å],[22] and Sn($NCPh_2$)$_4$ [2.068(37) Å].[23] Compound **6** also shows the typical cubic distortion observed in this class of compounds.

Compound **6** represents a rare example of a mixed-valent tin coordination complex possessing N-bridged Sn^{II} and Sn^{IV} centers; thus, the oxidation states of the respective Sn atoms were verified by solution-state ^{119}Sn NMR. It has been previously documented that both the oxidation state and coordination environment of the Sn atom influences ^{119}Sn NMR chemical shifts, with Sn^{II} centers typically exhibiting much larger downfield resonances.[24,25] Compound **6** possesses ^{119}Sn NMR resonances at δ −40.4 and 797, assigned

(19) Neumann, C.; Seifert, T.; Storch, W.; Vosteen, N.; Wrackmeyer, B. *Angew. Chem., Int. Ed.* **2001**, *40*, 3405−3407.
(20) Rannenberg, M.; Hausen, H. D.; Weidlein, J. *J. Organomet. Chem.* **1989**, *376*, C27−C30.
(21) Lappert, M. F.; Misra, M. C.; Onyszchuk, M.; Rowe, R. S.; Power, P. P.; Slade, M. J. *J. Organomet. Chem.* **1987**, *330*, 31−46.
(22) Laplaza, C. E.; Davis, W. M.; Cummins, C. *Organometallics* **1995**, *14*, 577−580.
(23) Alcock, N. W.; Pierce-Butler, M. *J. Chem. Soc., Dalton Trans.* **1975**, 2469−2476.
(24) Kennedy, J. D.; McFarlane, W. In *Multinuclear NMR*; Mason, J., Ed.; Plenum: New York, 1987; Chapter 4.
(25) Wrackmeyer, B. *Annu. Rep. NMR Spectrosc.* **1999**, *38*, 203.

Table 1. Crystal Data and Structure Refinement for Compounds **2**−**6**

	2	**3**	**4**	**5**	**6**
formula	$C_{20}H_{56}N_2O_2Li_2Ge_2Sn_2$	$C_{12}H_{36}N_4Ge_8$	$C_{12}H_{36}N_4Sn_4Ge_4$	$C_{12}H_{36}N_4Pb_4Ge_4$	$C_{12}H_{36}N_4Sn_8$
fw	753.11	817.17	1033.57	2674.85	1185.97
cryst dimens (mm)	0.32 × 0.27 × 0.19	0.17 × 0.14 × 0.10	0.19 × 0.09 × 0.07	0.37 × 0.14 × 0.12	0.14 × 0.10 × 0.10
cryst syst	tetragonal	cubic	monoclinic	cubic	cubic
space group	$P\bar{4}n2$	$I\bar{4}3m$	$C2/c$	$P\bar{4}3n$	$I\bar{4}3m$
a (Å)	9.7798(6)	11.2872(10)	12.520(4)	18.2282(14)	11.6106(14)
b (Å)	9.7798(6)	11.2872(10)	17.891(5)	18.2282(14)	11.6106(14)
c (Å)	17.664(2)	11.2872(10)	15.642(5)	18.2282(14)	11.6106(14)
α (deg)	90	90	90	90	90
β (deg)	90	90	107.536	90	90
γ (deg)	90	90	90	90	90
V (Å^3)	1689.4(3)	1438.0(2)	3341.1(17)	6056.6(8)	1565.2(3)
Z	2	2	4	4	2
D_{calcd} (g/cm^3)	1.480	1.887	2.055	2.933	2.516
T (K)	193(2)	193(2)	193(2)	193(2)	193(2)
μ (mm^{-1})	3.238	8.245	6.497	26.067	6.276
θ range (deg)	2.31−28.73	2.55−28.79	2.05−28.75	1.58−28.68	2.48−28.69
no. of reflns measd	9503	4569	10 311	36 464	4478
no. of indep reflns	2087	369	3989	2561	405
no. of reflns obsd	1828	329	1908	1359	394
no. of param used	80	18	130	73	18
index ranges	$-12 \le h \le 12$	$-14 \le h \le 15$	$-8 \le h \le 16$	$-21 \le h \le 23$	$-15 \le h \le 15 - 8 \le l \le 15$
	$-13 \le k \le 11$	$-12 \le k \le 15$	$-18 \le k \le 23$	$-23 \le k \le 24$	$-15 \le k \le 15$
	$-23 \le l \le 11$	$-15 \le l \le 14$	$-21 \le l \le 19$	$-14 \le l \le 23$	$-8 \le l \le 15$
R1 [$I > 2\sigma(I)$]	0.0385	0.0339	0.0865	0.0579	0.0214
wR2 [$I > 2\sigma(I)$]	0.0977	0.0757	0.2208	0.1416	0.0474
GOF	1.075	1.047	0.975	0.974	1.226
$\Delta\rho_{max}$ (e/Å^3)	0.616	0.785	4.388	2.855	0.915
min/max transm	0.5827/0.4211	0.4868/0.3346	0.6664/0.3763	0.5466/0.2102	0.5669/0.4823

Table 2. Selected Interatomic Distances (Å) and Angles (deg) for Compound **3**

Ge(1)−N(1)#1	2.002(4)	N(1)#1−Ge(1)−N(1)#2	84.0(3)
Ge(1)−N(1)#2	2.002(4)	N(1)#1−Ge(1)−N(1)#3	84.0(3)
Ge(1)−N(1)#3	2.002(4)	N(1)#2−Ge(1)−N(1)#3	84.0(3)
Ge(2)−N(1)	1.870(9)	Ge(2)−N(1)−Ge(1)#6	121.1(2)
Ge(2)−C(1)	1.937(7)	Ge(2)−N(1)−Ge(1)#7	121.1(2)
Ge(2)−C(1)#4	1.937(7)	Ge(1)#6−N(1)−Ge(1)#7	95.7(3)
Ge(2)−C(1)#5	1.937(7)	Ge(2)−N(1)−Ge(1)#8	121.1(2)
N(1)−Ge(1)#6	2.002(4)	Ge(1)#6−N(1)−Ge(1)#8	95.7(3)
N(1)−Ge(1)#7	2.002(4)	Ge(1)#7−N(1)−Ge(1)#8	95.7(3)
N(1)−Ge(1)#8	2.002(4)		

Table 3. Selected Interatomic Distances (Å) and Angles (deg) for Compound **4**

Sn(1)−N(1)	2.169(11)	Ge(2)−C(6)	1.91(2)
Sn(1)−N(2)#1	2.187(12)	Ge(2)−C(4)	2.032(18)
Sn(1)−N(2)	2.201(12)	N(1)−Sn(2)#1	2.235(11)
Sn(2)−N(1)	2.210(11)	N(2)−Sn(1)#1	2.187(12)
Sn(2)−N(2)#1	2.219(11)	N(2)−Sn(2)#1	2.219(11)
Sn(2)−N(1)#1	2.235(11)	N(1)−Sn(1)−N(2)#1	82.8(4)
Ge(1)−N(2)	1.855(12)	N(1)−Sn(1)−N(2)	83.5(4)
Ge(1)−C(2)	1.964(15)	N(2)#1−Sn(1)−N(2)	81.5(5)
Ge(1)−C(3)	1.977(17)	N(1)−Sn(2)−N(2)#1	81.2(4)
Ge(1)−C(1)	2.030(18)	N(1)−Sn(2)−N(1)#1	83.0(4)
Ge(2)−N(1)	1.865(12)	N(2)#1−Sn(2)−N(1)#1	81.6(4)
Ge(2)−C(5)	1.885(19)	Sn(1)−N(1)−Sn(2)	98.0(5)
Sn(1)−N(1)−Sn(2)#1	97.1(4)	Sn(1)#1−N(2)−Sn(2)#1	97.2(5)
Sn(2)−N(1)−Sn(2)#1	96.3(4)	Sn(1)−N(2)−Sn(2)#1	96.6(4)
Ge(1)−N(2)−Sn(1)#1	119.8(5)		
Sn(1)#1−N(2)−Sn(1)	98.2(5)		

Table 4. Selected Interatomic Distances (Å) and Angles (deg) for Compound **5**

Pb(1)−N(1)	2.303(14)	Ge(2)−C(3)	1.95(3)
Pb(1)−N(1)#1	2.303(14)	Ge(2)−C(4A)	2.04(5)
Pb(1)−N(1)#2	2.303(14)	Ge(2)−C(2)	2.42(10)
Pb(1)−Pb(1)#1	3.467(2)	N(1)−Pb(1)#1	2.303(14)
Pb(1)−Pb(1)#2	3.467(2)	N(1)−Pb(1)#2	2.303(14)
Pb(1)−Pb(1)#3	3.467(2)	N(2)−Pb(2)#4	2.291(15)
Pb(2)−N(2)	2.247(15)	N(2)−Pb(2)#6	2.293(16)
Pb(2)−N(2)#4	2.291(15)	N(1)−Pb(1)−N(1)#1	81.8(9)
Pb(2)−N(2)#5	2.293(16)	N(1)−Pb(1)−N(1)#2	81.8(9)
Pb(2)−C(3A)#5	2.73(15)	N(1)#1−Pb(1)−N(1)#2	81.8(9)
Pb(2)−Pb(2)#4	3.4525(15)	N(2)−Pb(2)−N(2)#4	80.1(7)
Pb(2)−Pb(2)#6	3.4718(13)	N(2)−Pb(2)−N(2)#5	80.5(7)
Pb(2)−Pb(2)#5	3.4718(13)	N(2)#4−Pb(2)−N(2)#5	79.6(7)
Ge(1)−N(1)	1.82(3)	Pb(1)−N(1)−Pb(1)#1	97.7(8)
Ge(1)−C(1)#7	1.96(3)	Pb(1)−N(1)−Pb(1)#2	97.7(8)
Ge(1)−C(1)#8	1.96(3)	Pb(1)#1−N(1)−Pb(1)#2	97.7(8)
Ge(1)−C(1)	1.96(3)	Pb(2)−N(2)−Pb(2)#4	99.1(6)
Ge(2)−N(2)	1.882(19)	Pb(2)−N(2)−Pb(2)#6	99.8(7)
Ge(2)−C(2A)	1.94(3)	Pb(2)#4−N(2)−Pb(2)#6	98.5(6)
Ge(2)−C(4)	1.95(5)		

Table 5. Selected Interatomic Distances (Å) and Angles (deg) for Compound **6**

Sn(1)−N(1)#1	2.196(3)	N(1)#1−Sn(1)−N(1)#2	83.1(2)
Sn(1)−N(1)#2	2.196(3)	N(1)#1−Sn(1)−N(1)	83.1(2)
Sn(1)−N(1)	2.196(3)	N(1)#2−Sn(1)−N(1)	83.1(2)
Sn(2)−N(1)	2.043(7)	Sn(2)−N(1)−Sn(1)	120.54(15)
Sn(2)−C(1)#4	2.139(5)	Sn(2)−N(1)−Sn(1)#1	120.54(15)
Sn(2)−C(1)	2.139(5)	Sn(1)−N(1)−Sn(1)#1	96.5(2)
Sn(2)−C(1)#5	2.139(5)	Sn(2)−N(1)−Sn(1)#2	120.54(15)
N(1)−Sn(1)#1	2.196(3)	Sn(1)−N(1)−Sn(1)#2	96.5(2)
N(1)−Sn(1)#2	2.196(3)	Sn(1)#1−N(1)−Sn(1)#2	96.5(2)

to the Sn^{IV} and Sn^{II} atoms, respectively, which are in agreement with the generally accepted ranges of tetra- and divalent ^{119}Sn NMR chemical shifts.[25] The endocube Sn^{II} shift is similar to that previously reported for $[Sn(\mu_3\text{-}NSiMe_3)]_4$ (δ 782),[8] though 161 ppm upfield from the resonance observed for compound **4** (δ 954). The lack of correlation between solution-state ^{119}Sn NMR chemical shifts and molecular structure, seen in the aforementioned series of tin cubanes, has been previously discussed in the literature.[26] The exocube Sn^{IV} shift in compound **6**, observed in the downfield region of the tetravalent Sn chemical shift range,

(26) Eichler, B. E.; Phillips, B. L.; Power, P. P.; Augustine, M. P. *Inorg. Chem.* **2000**, *39*, 5450−5453.

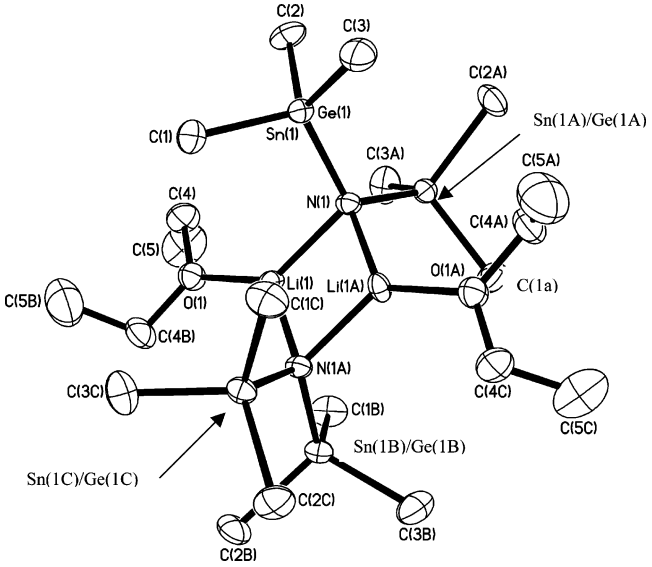

Figure 4. ORTEP plot representation (30% probability) with a numbering scheme for compound **2**. H atoms have been omitted for clarity.

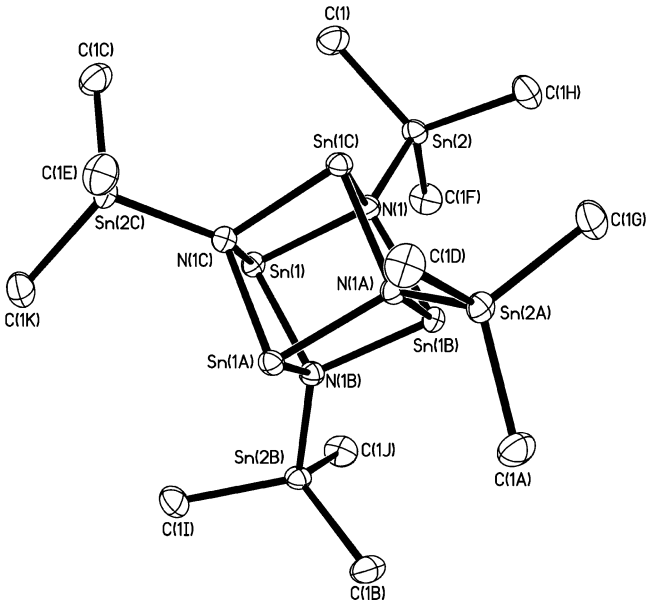

Figure 5. ORTEP plot representation (30% probability) with a numbering scheme for compound **6**. H atoms have been omitted for clarity.

is not unprecedented for a Sn center in this type of chemical environment [$Me_3SnN(SiMe_3)_2$, δ 55.3].[27] To our knowledge, the sulfito-bridged dicubane complex recently reported by Chivers et al.[4] represents the only other compound possessing N-bridged Sn^{II} and Sn^{IV} centers (though other examples of mixed-valent Sn species lacking N bridges have been reported[28]). Chivers' mixed-valent complex displays resonances at δ 490 and −258, attributed to the Sn^{II} and Sn^{IV} atoms, respectively. The pronounced upfield shift of the sulfito-bridged Sn^{IV} atom can be explained by the hexacoordination environment around this Sn center.

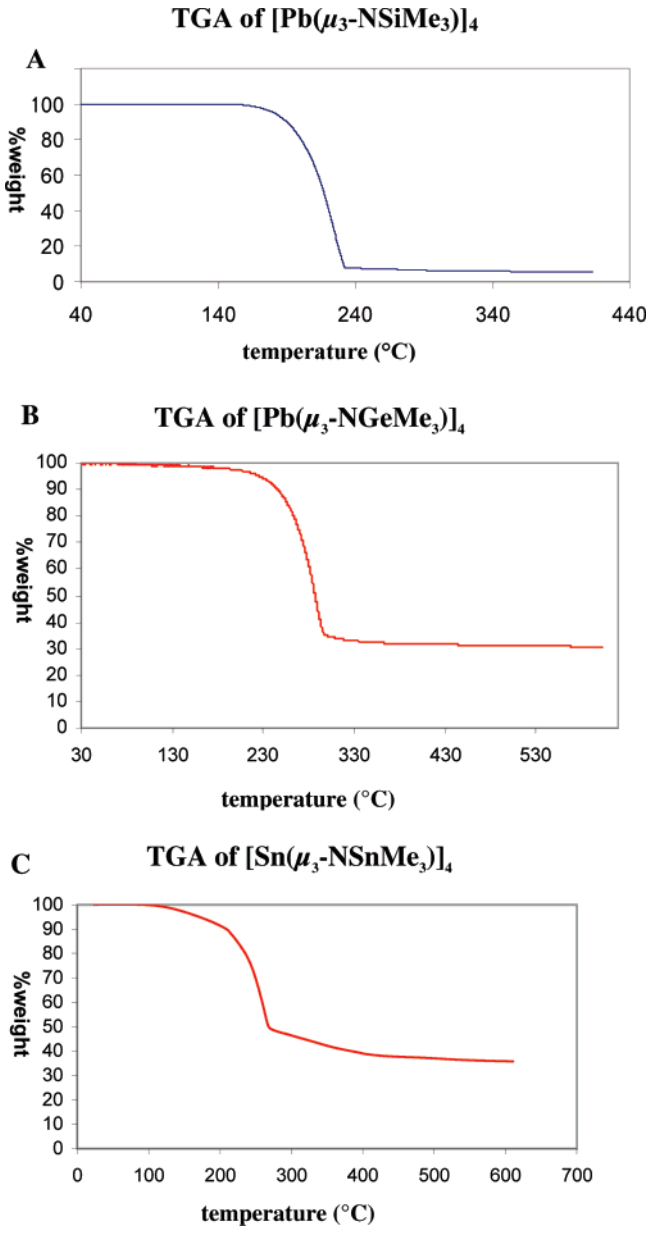

Figure 6. TGA plot of percent weight vs temperature for [$Pb(\mu_3$-$NSiMe_3)]_4$ (A), compound **4** (B), and compound **6** (C).

Chivers and co-workers have also discussed the potential application of group 14 M−N heterocubanes as precursors for IV−VI semiconductor materials.[3] On the basis of the previous successful employment of metal amides in MOCVD processes,[13,14] an evaluation of the precursor suitability for the tetrameric cubane complexes **5** and **6** and the previously synthesized [$Pb(\mu_3$-$NSiMe_3)]_4$ was warranted. Earlier work by Barron and co-workers suggested that the heterocubane geometrical motif could lend unexpected thermal stability and vapor-phase integrity to oligomeric species.[29] This notion is corroborated by the results presented here. TGA studies indicate that the Pb−N heterocubanes [$Pb(\mu_3$-$NSiMe_3)]_4$ and [$Pb(\mu_3$-$NGeMe_3)]_4$ (**5**) are more thermally stable than compound **6**, evidenced by the single-step mass loss for the Pb

(27) Rannenberg, M.; Weidlein, J. *Z. Naturforsch.* **1991**, *46b*, 459−467.
(28) (a) Boegeat, D.; Jousseaume, B.; Toupance, T.; Campet, G.; Fournes, L. *Inorg. Chem.* **2000**, *39*, 3924−3927. (b) Eichler, B. E.; Power, P. P. *Inorg. Chem.* **2000**, *39*, 5444−5449. (c) Cardin, C. J.; Cardin, D. J.; Constantine, S. P.; Todd, A. K. *Organometallics* **1998**, *17*, 2144−2146.
(29) MacInnes, A. N.; Power, M. B.; Barron, A. R. *Chem. Mater.* **1992**, *4*, 11−14.

congeners (Figure 6). This is not entirely unexpected because Pb is more stable in the 2+ oxidation state than Sn. In addition, the Pb complex possessing exocube trimethylsilyl substituents displays higher volatility and thermal stability than the corresponding complex with trimethylgermyl substituents, presumably because of its lower molecular weight and the presence of labile Ge−N linkages in **5**.

In conclusion, the present report documents the generality of the route to divalent group 14 imidocubanes that proceeds via the reaction of lithiated stannylamines and divalent metal halides. This synthetic pathway readily affords group 14 M−N heterocubanes that possess unusually heavy exocube substituents. In addition, compounds **3** and **5** augment the narrow library of structurally characterized germanium(II) and lead(II) imidocubanes, and complexes **3** and **6** represent rare examples of compounds containing N-bridged Ge^{II}/Ge^{IV} and Sn^{II}/Sn^{IV} centers, respectively. Finally, on the basis of the initial TGA studies, this structural motif provides access to volatile compounds potentially applicable as MOCVD precursors.

Acknowledgment. We gratefully acknowledge partial support of this project by the Georgia Institute of Technology Molecular Design Institute, under prime Contract N00014-95-1-1116 from the Office of Naval Research.

Supporting Information Available: Crystallographic data (CIF format) and ORTEP plot of **1**. This material is available free of charge via the Internet at http://pubs.acs.org.

IC060331Y